チル-D-アスパラギン酸）レセプターも活性化されることが証明された。この新たに活性化されたNMDAレセプターを介する神経活動が、耳鳴の原因であるという説である。NMDAレセプターの阻害薬が耳鳴を軽減するとの臨床報告もある[14]。すなわち、通常の外界からの音を感知する場合はAMPAレセプターが働き、耳鳴の場合はNMDAレセプターが働くということになる。この説に従うと、今回の報告のMCL・UCL検査ではAMPAレセプター、耳鳴ではNMDAレセプターが関与することになり、NMDA関与の耳鳴をTRTで順応させても、AMPA関与のMCL・UCL検査はTRTで影響を受けなかったと考えられる。

文 献

1) Jastreboff PJ：Phantom auditory perception (tinnitus) — Mechanisms of generation and perception —. Neurosci Res **8**：221-254, 1990.
2) 関谷芳正他：耳鳴に対する新しい治療法・TRT（療法）．耳鼻臨床 **95**：639-646, 2002.
3) 君付 隆他：MCL・UCL検査の判定基準．耳鼻 **54**：140-145, 2008.
4) 耳鳴研究会：標準耳鳴検査法1993．耳鳴の検査．立木孝・曽田豊二編，111-116頁，金原出版，東京，1999.
5) 高橋真理子・村上信五：耳鳴治療のための耳鳴評価法．ENTONI **49**：34-39, 2000.
6) Newman CW et al：Psychometric adequancy of the Tinnitus Handicap Inventory (THI) for evaluating treatment outcome. J Am Acad Audiol **9**：153-160, 1998.
7) Vernon JA and Meikle MB：Tinnitus clinical measurement. Otolaryngol Clin North Am **36**：293-305, 2003.
8) Feldmann H：Homolateral and contralateral masking of tinnitus by noise-bands and pure tones. Audiology **10**：138-144, 1971.
9) Sammeth CA et al：Variability of most comfortable and uncomfortable loudness levels to speech stimuli in the hearing impaired. Ear Hear **10**：94-100, 1989.
10) 新谷朋子他：耳鳴と聴覚過敏．JOHNS **23**：15-18, 2007.
11) Tonndorf J：Stereociliary dysfunction, a cause of sensory hearing loss, recruitment, poor speech discrimination and tinnitus. Acta Otolaryngol **91**：469-479, 1981.
12) Guitton MJ et al：Salicylate induced tinnitus through activation of cochlear NMDA receptors. J Neurosci **23**：3944-3952, 2003.
13) Ruel J et al：Salicylate enables cochlear arachidonic-acid-sensitive NMDA receptor responses. J Neurosci **28**：7313-7323, 2008.
14) Figueiredo RR et al：Tinnitus treatment with memantine. Otolaryngol Head Neck Surg **138**：492-496, 2008.

（受付 2010年4月26日）

Changes in the MCL/UCL test for patients undergoing Tinnitus retraining therapy (TRT)

Takashi KIMITSUKI, Nozomu MATSUMOTO, Shumei SHIBATA, Akihiro TAMAE, Mitsuru OHASHI, Yoshihiro UMENO, Atsuko NOGUCHI, Kazuha HORIKIRI and Shizuo KOMUNE

Department of Otorhinolaryngology, Graduate School of Medical Sciences, Kyushu University, Fukuoka 812-8582, Japan

Tinnitus retraining therapy (TRT) has become a popular treatment for the treatment of patients with tinnitus. This method involves the habituation of tinnitus perception using a low level sound generator and directive counseling. In this paper, we examined whether the most comfortable loudness level (MCL) and uncomfortable loudness level (UCL) changed after undergoing TRT. Nine patients (four males, five females) underwent TRT for 4-22 months (for an average of 12 months). The tinnitus handicap inventory (THI) score improved from 59.7 to 20.2, but neither the MCL nor the UCL showed any changes after TRT. In one patient where the UCL was particularly low prior to treatment, no changes were observed in either MCL or UCL after TRT.

Hearing Research 261 (2010) 57–62

Contents lists available at ScienceDirect

Hearing Research

journal homepage: www.elsevier.com/locate/heares

Research paper

Property of $I_{K,n}$ in inner hair cells isolated from guinea-pig cochlea

Takashi Kimitsuki *, Noritaka Komune, Teppei Noda, Kazutaka Takaiwa, Mitsuru Ohashi, Shizuo Komune

Department of Otolaryngology, Graduate School of Medical Sciences, Faculty of Medicine, Kyushu University, 3-1-1 Maidashi, Higasi-Ku, Fukuoka 812-8582, Japan

ARTICLE INFO

Article history:
Received 12 September 2009
Received in revised form 4 January 2010
Accepted 5 January 2010
Available online 12 January 2010

Keywords:
Cochlea
Inner hair cell
Potassium currents
KCNQ-channel
Linopirdine
XE991

ABSTRACT

One of the potassium currents, $I_{K,n}$, is already activated at the resting potential of the cell and thus determines the membrane potential. KCNQ4 channel has been identified as the molecular correlate of $I_{K,n}$. In the present study, we measured $I_{K,n}$ in acutely isolated IHCs of guinea-pig cochlea using the whole-cell voltage-clamp techniques, and investigated the properties of the currents. $I_{K,n}$ was 70% activated around the resting potential of −60 mV and deactivated on hyperpolarization. $I_{K,n}$ was blocked by the KCNQ-channel blockers, linopirdine (100 μM) and XE991 (10 μM), but was insensitive to both $I_{K,f}$ blocker, tetraethylammonium (TEA), and $I_{K,s}$ blocker, 4-aminopyridine (4-AP). There was no significant difference in the size of $I_{K,n}$ between the apical and basal turn IHCs.

1. Introduction

In the mammalian cochlea, there are two types of hair cells that subserve distinct functions and receive characteristic patterns of innervations. Inner hair cells (IHCs) receive nearly all the afferent innervations and are primary acoustic transducers. The three IHC potassium currents are distinguishable by their pharmacology and their activation kinetics (Kros and Crawford, 1990; Marcotti et al., 2003). The fast activating current, $I_{K,f}$, is blocked by TEA but resistant to 4-AP. $I_{K,s}$ is activated more slowly on depolarization and is blocked by 4-AP but not by TEA. Another potassium current, $I_{K,n}$, is already activated at the resting potential of the cell and thus determines the membrane potential and membrane constant (Housley and Ashmore, 1992; Nakagawa et al., 1994; Marcotti and Kros, 1999). Initially $I_{K,n}$ was identified in outer hair cells (OHCs) (Housley and Ashmore, 1992). Although there is no detectable expression of KCNQ4, which is thought to constitute the major conductance $I_{K,n}$, in IHCs (Beisel et al., 2000; Kharkovets et al., 2000), a recent article suggested that KCNQ4 is expressed in IHCs (Oliver et al., 2003). This current has recently been implicated in developmental changes in IHCs during the postnatal days just preceding functional maturation of hearing in mice (Kros et al., 1998; Marcotti et al., 2003).

$I_{K,n}$ in IHCs has been identified and characterized in mice previously (Oliver et al., 2003; Marcotti et al., 2003), however, it is important to confirm this current in guinea-pig, which is a commonly used model. In the present study, we isolated the IHCs from mature guinea-pig cochlea and investigated the properties of $I_{K,n}$ such as the K blocker effect and the activation properties. Tonotopic differences of $I_{K,n}$ in the cochlear turn were also investigated.

2. Material and methods

2.1. Preparation of isolated IHCs

An adult albino guinea-pig (200–350 g, 3–6 weeks) was killed by rapid cervical dislocation, both bullae were removed and the cochlea exposed. The cochlea, fused to the bulla, was placed in a Ca^{2+}-free external solution (mM: 142 NaCl, 4 KCl, 3 $MgCl_2$, 2 NaH_2PO_4, 8 Na_2HPO_4, adjusted to pH 7.4 with NaOH). The otic capsule was opened, allowing removal of the organ of Corti attached to the modiolus. IHCs were isolated by micro-dissecting a selected turn of the organ of Corti; from turn 1–2 (basal portion) and turn 4 (apical portion). The organ of Corti was treated with trypsin (0.5 mg/ml, T-4665, Sigma) for 12 min, and gentle mechanical trituration was carried out. Trypsin was rinsed from the specimen by superfusing with a standard external solution (mM: 142 NaCl, 4 KCl, 2 $MgCl_2$, 1 $CaCl_2$, 2 NaH_2PO_4, 8 Na_2HPO_4, adjusted to pH 7.4 with NaOH) for at least 10 min before starting any experiments. The most important landmarks for identifying IHCs are a tight neck and angle between the cuticular plate and the axis of the cell as

Abbreviations: IHC, inner hair cell; OHC, outer hair cell; TEA, tetraethylammonium; 4-AP, 4-aminopyridine; CAP, compound action potential

* Corresponding author. Tel.: +81 92 642 5668; fax: +81 92 642 5685.
E-mail address: kimitaka@qent.med.kyushu-u.ac.jp (T. Kimitsuki).

0378-5955/$ - see front matter © 2010 Elsevier B.V. All rights reserved.
doi:10.1016/j.heares.2010.01.002

described previously (He et al., 2000; Yang et al., 2002; Kimitsuki et al., 2009).

2.2. Recording procedures

Membrane currents were measured by conventional whole-cell voltage-clamp recordings using an EPC-10 (HEKA, Lambrecht, Germany). Data acquisition was controlled by the software PatchMaster (HEKA, Lambrecht, Germany). Recording electrodes were pulled on a two-stage vertical puller (PP830 Narishige, Tokyo, Japan) using 1.2 mm outside diameter borosilicate glass (GC-1.2, Narishige, Tokyo) filled with an internal solution (mM: 144 KCl; 2 $MgCl_2$; 1 NaH_2PO_4; 8 Na_2HPO_4; 2 ATP; 3 D-glucose; 0.5 EGTA; adjusted to pH 7.4 with KOH.). Pipettes showed a resistance of 4–8 MΩ in the bath and were coated with ski wax (Tour-DIA, DIAWax, Otaru, Japan) to minimize capacitance. The cell's capacitance was 9.6 ± 3.0 pF (mean ± SD) and the series resistance was 16.4 ± 6.1 MΩ (n = 16). Tetraethylammonium (TEA, T-2265, Sigma), 4-aminopyridine (4-AP, A-0152, Sigma), Linopirdine (L-134, Sigma), XE991 (No. 2000, Tocris), replacing an equivalent amount of NaCl in the standard external solution, was applied under pressure (Pressure micro-injector: PMI-200, Dagan, Minneapolis) using pipettes with a tip diameter of 2–4 μm positioned around 50 μm from the IHCs. Cells were continuously perfused with external saline and all experiments were performed at room temperature (20–25 °C).

2.3. Animal care

The experimental design was reviewed and approved (Accession No. A19-104-0) by the Animal Care and Use Committee, Kyushu University. All procedures were conducted in accordance with the Guidelines for Animal Care and Use Committee, Kyushu University.

3. Results

3.1. $I_{K,n}$ activated at resting potentials

Currents in response to hyperpolarizing and depolarizing voltage steps from a holding potential of −60 mV were recorded from IHCs. Typical current records are shown in Fig. 1A. IHCs had outwardly rectifying currents ($I_{K,f}$) in response to depolarizing voltage pulses, with only a slight inward current when hyperpolarized. Fig. 1B demonstrated the inward components by enlarging the scale. Sizeable currents were detected as decaying inward currents that commenced instantaneously when the membrane was stepped below −90 mV. At hyperpolarized potentials the decay time of the transient, indicating the channel deactivation, varied considerably depending on membrane potentials. These deactivating inward currents corresponded to $I_{K,n}$ previously found in OHCs (Housley and Ashmore, 1992; Nakagawa et al., 1994; Marcotti and Kros, 1999) and immature IHCs (Kros et al., 1998; Marcotti et al., 2003) already activated at resting potentials.

3.2. voltage-dependent activation of $I_{K,n}$

The voltage-dependent activation of $I_{K,n}$ was examined by analyzing the peak of the tail currents at a fixed membrane potential of −160 mV, following depolarizing and hyperpolarizing voltage steps. In most cases, the tail currents observed from large hyperpolarizing steps (−140 to −160 mV) overlapped, suggesting that $I_{K,n}$ was fully turned off at these negative potentials. Conversely, there was overlap of the traces when the pre-pulse was greater than −20 mV, which is interpreted as complete activation of the current. Fig. 2 shows an activation curve derived for $I_{K,n}$, fitted by first-order Boltzmann equation:

$$I/I_{max} = 1/[1 + \exp((V_{half} - V)/S)]$$

where V_{half} is the potential of half-maximal activation, V is the membrane potential of the preceding voltage step and S describes the voltage sensitivity of activation. Fitting was performed by using the average values (filled squares) at various membrane potentials in 10 cells. V_{half} and S were −84.5 mV and 25.3 mV, respectively.

3.3. K channel blocker effect to $I_{K,n}$

The fast activating current, $I_{K,f}$, is blocked by TEA and slow activating current, $I_{K,s}$, is blocked by 4-AP. The effects of 25 mM TEA (Fig. 3A) and 30 mM 4-AP (Fig. 3B) were investigated. Both K channel blockers reduced the amplitude of outward-going currents (insets in Fig. 3A showed the TEA block onto the fast activating $I_{K,f}$) but did not affect the inward currents, suggesting that $I_{K,n}$ is insensitive to TEA and 4-AP. KCNQ4 channel has been identified as the molecular correlate of the $I_{K,n}$ in OHCs (Marcotti and Kros, 1999)

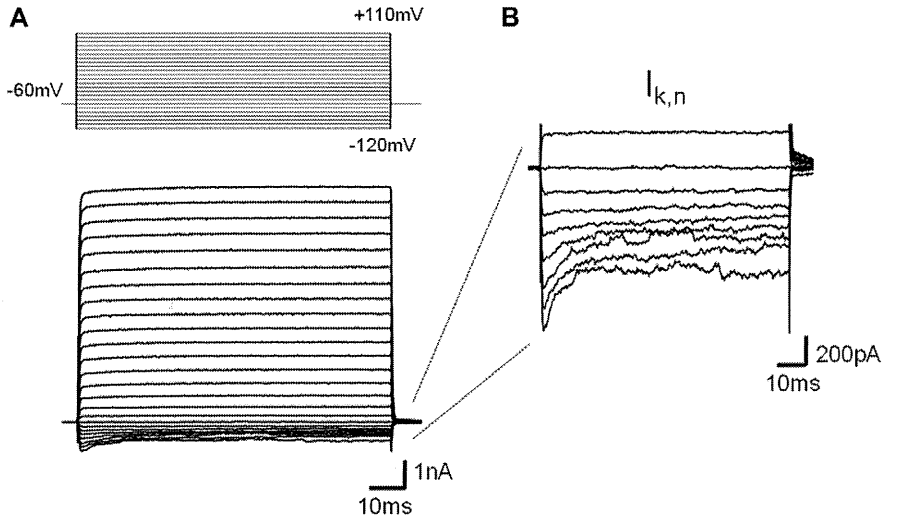

Fig. 1. $I_{K,n}$ activated at resting potentials. Currents in response to hyperpolarizing and depolarizing voltage steps from a holding potential of −60 mV (A, lower panel). Voltage protocol (A, upper panel). The inward component of the currents by enlarging the scale (B).

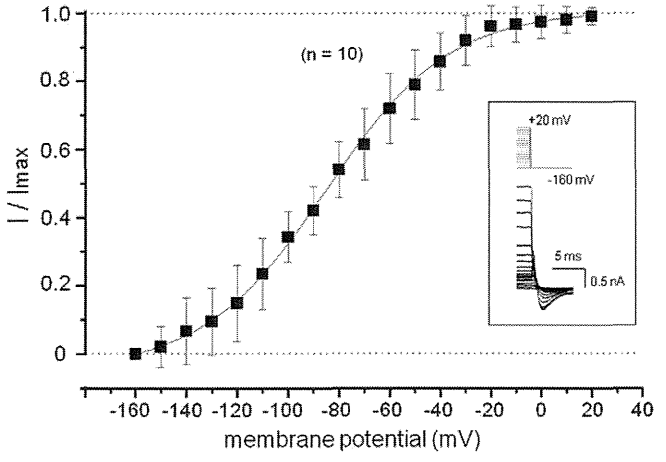

Fig. 2. Voltage-dependent activation of $I_{K,n}$. The voltage-dependent activation was evaluated by analyzing the tail currents at a fixed membrane potential of −160 mV, following depolarizing and hyperpolarizing voltage steps (inset). An activation curve derived from $I_{K,n}$ fitted by first-order Boltzmann equation: $I/I_{max} = 1/[1 + \exp((V_{half} - V)/S)]$. V_{half} and S were −84.5 mV and 25.3 mV, respectively.

and IHCs (Oliver et al., 2003), so we used the KCNQ-channel blocker linopirdine and XE991 to examine whether they block the currents. Inward currents were obviously blocked by 100 μM linopirdine (Fig. 4A) and 10 μM XE991 (Fig. 4B). In contrast, outward currents were not changed by either linopirdine or XE991, suggesting that only inward currents consist of $I_{K,n}$. In linopirdine solutions, four out of five cells showed the inward current depression, and in XE991 solutions, three out of four cells showed the inward current depression.

3.4. Amplitude of $I_{K,n}$ in apical and basal turn IHCs

A comparison of the amplitude of $I_{K,n}$ recorded from apical and basal turn IHCs is shown in Fig. 5. The amplitudes of inward currents at −130 mV were measured from seven apical cells and five basal cells, and shown as a boxplot. Minimum value (×), 25th percentile line, median line, 75th percentile line and maximum value (×) were shown. Mean (open square) ± standard deviation were 377 ± 192 pA and 338 ± 113 pA in apical and basal IHCs, respectively, showing that there was no difference between apical and basal turn IHCs in $I_{K,n}$ amplitude ($P = 0.65$ in analysis of variance: ANOVA). The cell capacitances were 9.3 ± 3.0 pF and 9.0 ± 3.5 pF in apical and basal IHCs, respectively, suggesting that current density is not different for the two tonotopic locations. Maximum currents from tails (fixed at −160 mV) were compared to avoid the influence of open probability. Mean ± standard deviation were 146 ± 62 pA ($n = 4$) and 154 ± 66 pA ($n = 3$) in apical and basal turn, respectively, suggesting that the voltage dependence of this current is independent of tonotopic location.

4. Discussion

Using whole-cell voltage-clamp recordings, we studied the $I_{K,n}$ in acutely isolate IHCs of guinea-pig cochlea. $I_{K,n}$ was 70% activated at around the resting potential of −60 mV and deactivated on hyperpolarization (Fig. 2). $I_{K,n}$ was blocked by the KCNQ-channel blockers linopirdine and XE991 but was insensitive to TEA and 4-AP (Figs. 3 and 4). There was no significant difference in the size of $I_{K,n}$ between the apical turn and basal turn.

Recently, mutations in the KCNQ4 K^+ channel gene have been shown to underlie the progressive autosomal dominant hearing loss classified as DFNA2 (Kubisch et al., 1999). KCNQ4 is expressed in the basolateral membrane of cochlear outer hair cells (OHCs) and is thought to constitute the major OHC K^+ conductance $I_{K,n}$ (Housley and Ashmore, 1992; Marcotti and Kros, 1999; Kharkovets et al., 2000). To date, expression of KCNQ4 has been thought to be restricted to cochlear OHCs, vestibular hair cells, and central auditory neurons (Kubisch et al., 1999; Kharkovets et al., 2000). However, recent reports demonstrated the expression of KCNQ4 in IHCs of mice using immunofluorescence (Oliver et al., 2003) or *in situ* hybridization and RT-PCR analysis (Beisel et al., 2000). The

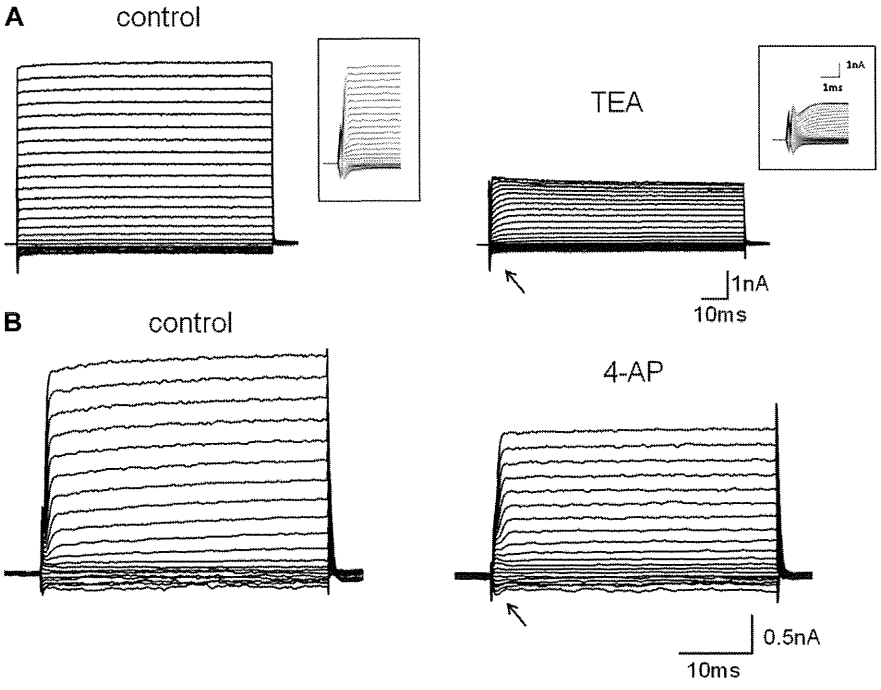

Fig. 3. TEA and 4-AP effects on $I_{K,n}$. The outward currents were blocked by 25 mM TEA (A) and 30 mM 4-AP (B). Inward currents were insensitive to both TEA and 4-AP (arrows). *Insets* in Fig. 3A showed the expanded time scale in the activating phase of the currents. TEA blocked the fast activating outward $I_{K,f}$.

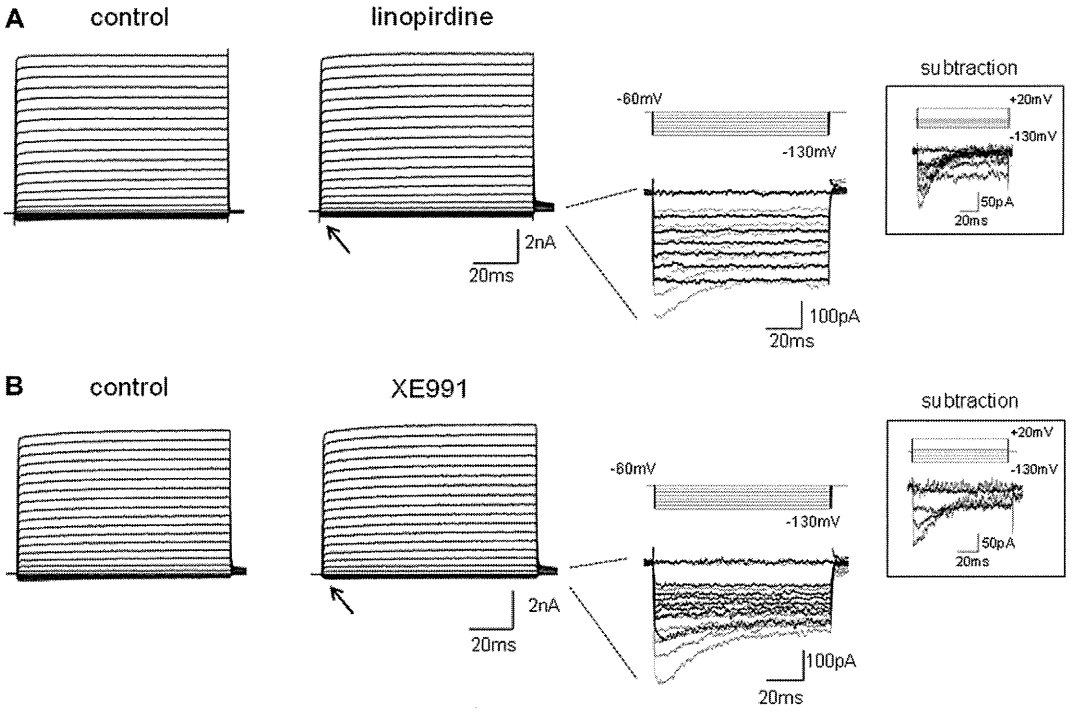

Fig. 4. Linopirdine and XE991 effects to $I_{K,n}$. Inward currents were blocked by the KCNQ-channel blocker 100 μM linopirdine (A) and 10 μM XE991 (B). Inward currents are shown by enlarging scale (right panel). Gray traces indicate control currents and black traces indicate $I_{K,n}$ with linopirdine or XE991. Insets showed the linopirdine- or XE991-sensitive currents by subtracting blocker traces from controls.

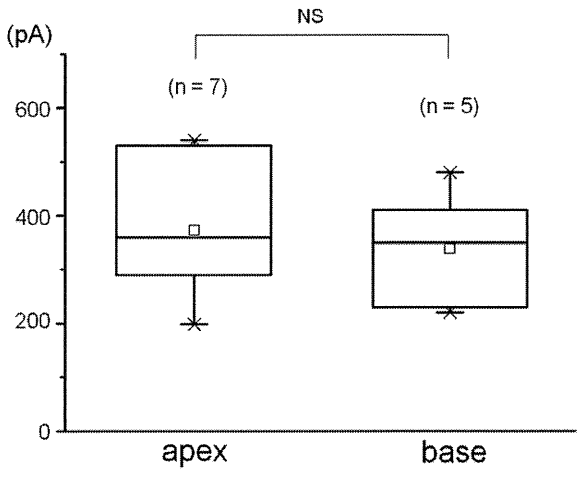

Fig. 5. Comparison between the amplitudes of $I_{K,n}$ in apical and basal turn IHCs. The amplitudes of inward currents at −130 mV were compared. Minimum value (×), 25th percentile line, median line, 75th percentile line and maximum value (×) were shown. Open squares indicate the mean values in the apical (377 pA) and basal turn (338 pA).

size of $I_{K,n}$ of IHCs was 45% of that of OHCs on comparison of 264 pA in IHCs (at a membrane potential of −124 mV: Marcotti et al., 2003) and 584 pA in OHCs (Marcotti and Kros, 1999). The amplitude of $I_{K,n}$ at −130 mV was 358 pA (Fig. 5, $n = 12$) in the present data, which is slightly larger than that in the previous report. The size of $I_{K,n}$ of IHCs was 61% of that of OHC, that is matching the respective sizes of the transducer conductance of IHCs and OHCs (Kros et al., 1992).

In the present study, trypsin was used and mechanical trituration was carried out to isolate the IHCs. Trypsin diminished the inactivation of BK channel (Kimitsuki et al., 2005) by attacking the N-terminal cytosolic hydrophobic peptide segments of auxiliary β subunit (Zhang et al., 2009). However, $I_{K,n}$ from the isolated IHCs, which is similar to that from the semi-intact preparation (Marcotti et al., 2003; Oliver et al., 2003), suggested that trypsin and trituration is inconsequential.

The first sign of $I_{K,n}$ was seen at postnatal day 12 (P12) in mouse IHCs (Marcotti et al., 2003), when the one-to-one axosomatic configuration between afferent fibers and IHCs found in mature synapses is established and the hearing onset occurs. The amplitude of $I_{K,n}$ increased and reached the maximum level at around P20. In the immunofluorescence study, KCNQ4 expression was observed initially around embryonic day 18.5 (E18.5) in the basal turn and proceeded longitudinally toward the apex (Beisel et al., 2000). At P8, the basal hook region showed the adult expression pattern and developmental upregulation had reached the apical turn. At P21, all hair cells, except those in the apical tip, had acquired the adult pattern. In the present study, $I_{K,n}$ was recorded from adult guinea-pigs, so the amplitude was slightly larger compared to the previous report (Marcotti et al., 2003).

There was a significant difference in the size of $I_{K,n}$ between the apical and basal turn IHCs in mice, showing larger $I_{K,n}$ in apical IHCs than that in basal IHCs (Marcotti et al., 2003). However, the resting membrane potential, that is mainly established by $I_{K,n}$, was similar in apical and basal IHCs. In contrast, the highest expression levels of KCNQ4 were found in the basal turn (Beisel et al., 2000), those findings contradicted the electrophysiological findings (Marcotti et al., 2003). Beisel et al. observed the longitudinal expression in the KCNQ4 protein by immunofluorescence technique, but they could not clarify the function of KCNQ4 K^+ channel. In the present study, there were no significant differences in $I_{K,n}$ amplitude between apical and basal turn IHCs (Fig. 5). This discrepancy might be due to the difference of species.

KCNQ K^+-channel blocker linopirdine has been a useful tool to define heterologous and native KCNQ currents (Wang et al., 1998; Kubisch et al., 1999; Lerche et al., 2000; Schroeder et al., 2000). The inward currents were insensitive to TEA and 4-AP but obviously blocked by the linopirdine (Fig. 4A) and XE991

(Fig. 4B). In mouse IHCs, blockage of $I_{K,n}$ by linopirdine was dose-dependent and slowly reversible with an IC_{50} of 0.58 μM (Oliver et al., 2003) or 0.56 μM (Marcotti et al., 2003). The concentration used in the present study was sufficient to block $I_{K,n}$ completely. *In vivo* study for guinea-pig, linopirdine significantly increased the threshold of the compound action potential (CAP) with an IC_{50} of 101 μM (Nouvian et al., 2003). They indicated that there was no recovery of CAP threshold after rinsing the cochlea with control artificial perilymph solutions. The blocking effect of another KCNQ-channel blocker XE991 for $I_{K,n}$ was described in mouse IHCs (Oliver et al., 2003). Sensitivity to XE991 was even higher than that to linopirdine because 100 nM blocked 77% of the current, and XE991-induced inhibition was irreversible contrary to the effect of linopirdine. XE991 block for KCNQ-channel was clearly demonstrated in OHCs in wild mouse ($Kcnq4^{+/+}$) but XE991-sensitive component was significantly reduced in $Kcnq4^{+/-}$ mice and was completely abolished in $Kcnq4^{-/-}$ mice (Kharkovets et al., 2006).

$I_{K,n}$, although small compared to the other outward currents $I_{K,f}$ and $I_{K,s}$, plays an important role close to the resting membrane potential because it showed around 70% activity in the present study (Fig. 2). $I_{K,n}$ provides a large K^+ conductance at the resting potential, and thus determines the membrane potential and membrane time constant (Housley and Ashmore, 1992; Marcotti and Kros, 1999). Although the $I_{K,f}$ blocker TEA did not change the resting potential (Oliver et al., 2003; Kros and Crawford, 1990) and the $I_{K,s}$ blocker 4-AP slightly shifted the resting potentials (Kros and Crawford, 1990), the $I_{K,n}$ blocker linopirdine markedly shifted the resting potentials toward a depolarization direction (Marcotti et al., 2003). Thus, $I_{K,n}$ sets the resting membrane potential and consequently maintains the intracellular Ca^{2+} at a low level by keeping the Ca^{2+} channels on closed state (Oliver et al., 2003). Another role of $I_{K,n}$ is the efflux route of K^+ ions to the perilymphatic space and prevention of K^+ accumulation in the cells. In OHCs, $I_{K,n}$ channels are located at the basolateral membrane facing the perilymphatic space (Nakagawa et al., 1994). Loss of this conductance in KCNQ4/DFNA2 patients is considered to impair K^+ efflux from OHCs, leading to degeneration of OHCs (Jentsch, 2000; Kharkovets et al., 2000). $I_{K,n}$ may also be important in IHCs to provide an exit route for K^+ ions entering through the mechano-electrical transducer channels.

KCNQ4 channels have been associated with the nonsyndromic dominant deafness DFNA2 (Kubisch et al., 1999; Talebizadeh et al., 1999; Van Hauwe et al., 2000; Van Camp et al., 2002). DFNA2 is characterized by a slowly progressive hearing loss that develops from high to low frequencies and finally leads to severe deafness (Marres et al., 1997; De Leenheer et al., 2002). In knockout and knock-in mouse, the hearing loss in DFNA2 is predominantly caused by the slow degeneration of OHCs due to chronic depolarization (Kharkovets et al., 2006), but complete loss of OHCs will ultimately reduce the hearing threshold by 40–50 dB (Ryan and Dallos, 1975). Although the loss of OHCs is compatible with DFNA2 hearing loss in its early stages, profound hearing loss in DFNA2 at the later age is insufficiently explained by nonfunctional OHCs. There might be an additional impairment of IHCs at the age when presbyacusis sets in. Destabilization of the resting potential and increase intracellular Ca^{2+}, which may be caused by impaired KCNQ4 function in IHCs, may promote the progressive hearing loss observed in DFNA2 patients. KCNQ4 is also expressed in spiral ganglion neurons (Beisel et al., 2005), and the nuclei of many neurons in the central auditory pathway, e.g., in the cochlear nuclei, nuclei of the lateral lemniscus, and the inferior colliculus (Kharkovets et al., 2000). The profound deafness in DFNA2 patients may be due to the later dysfunction of the KCNQ4 channels expressed in the nuclei and tracts of the central auditory pathway.

Acknowledgements

This work was supported by a Grant-in-Aid for Scientific Research 9591978, 21592160 from the Ministry of Education, Culture, Sports, Science and Technology of Japan and the Research Fund of Institute of Kampo Medicine (Japan).

References

Beisel, K.W., Nelson, N.C., Delimont, D.C., Fritzsch, B., 2000. Longitudinal gradients of KCNQ4 expression in spinal ganglion and cochlear hair cells correlate with progressive hearing loss in DFNA2. Brain Res. Mol. Brain Res. 82, 137–149.

Beisel, K.W., Rocha-Sanchez, S.M., Morris, K.A., Nie, L., Feng, F., Kachar, B., Yamoah, E.N., Fritzsch, B., 2005. Differential expression of KCNQ4 in inner hair cells and sensory neurons is the basis of progressive high-frequency hearing loss. J. Neurosci. 25, 9285–9293.

De Leenheer, E.M., Huygen, P.L., Coucke, P.J., Admiraal, R.J., van Camp, G., Cremers, C.W., 2002. Longitudinal and cross-sectional phenotype analysis in a new, large Dutch DFNA2/KCNQ4 family. Ann. Otol. Rhinol. Laryngol. 111, 267–274.

He, D.Z.Z., Zheng, J., Edge, R., Dallos, P., 2000. Isolation of cochlear inner hair cells. Hear. Res. 145, 156–160.

Housley, G.D., Ashmore, J.F., 1992. Ionic currents of outer hair cells isolated from guinea pig cochlea. J. Physiol. 448, 73–98.

Jentsch, T.J., 2000. Neuronal KCNQ potassium channels: physiology and role in disease. Nat. Rev. Neurosci. 1, 21–30.

Kharkovets, T., Hardelin, J.P., Safielddine, S., Schweizer, M., El-Amraoui, A., Petit, C., Jentsch, T.J., 2000. KCNQ4, a K^+ channel mutated in a form of dominant deafness, is expressed in the inner ear and the central auditory pathway. Proc. Natl. Acad. Sci. USA 97, 4333–4338.

Kharkovets, T., Dedek, K., Maier, H., Schweizer, M., Khimich, D., Nouvian, R., Vardanyan, V., Leuwer, R., Moser, T., Jentsch, T.J., 2006. Mice with altered KCNQ4 K+ channels implicate sensory outer hair cells in human progressive deafness. EMBO J. 25, 642–652.

Kimitsuki, T., Ohashi, M., Wada, Y., Fukudome, S., Komune, S., 2005. Dissociation enzyme effects on the potassium currents of inner hair cells isolated from guinea-pig cochlea. Hear. Res. 199, 135–139.

Kimitsuki, T., Kakazu, Y., Matsumoto, N., Noda, T., Komune, N., Komune, S., 2009. Salicylate-induced morphological changes of isolated inner hair cells and outer hair cells from guinea-pig cochlea. Auris Nasus Larynx 36, 152–156.

Kros, C.J., Crawford, A.C., 1990. Potassium currents in inner hair cells isolated from the guinea-pig cochlea. J. Physiol. 421, 263–291.

Kros, C.J., Rusch, A., Richardson, G.P., 1992. Mechano-electrical transducer currents in hair cells of the cultured neonatal mouse cochlea. Proc. R. Soc. Lond. 249, 185–193.

Kros, C.J., Ruppersberg, J.P., Rusch, A., 1998. Expression of a potassium current in inner hair cells during development of hearing in mice. Nature 394, 281–284.

Kubisch, C., Schroeder, B.C., Friedrich, T., Lutjohann, B., El-Amraoui, A., Marlin, S., Petit, C., Jentsch, T.J., 1999. KCNQ4, a novel potassium channel expressed in sensory outer hair cells, is mutated in dominant deafness. Cell 96, 437–446.

Lerche, C., Scherer, C.R., Seebohm, G., Derst, C., Wei, A.D., Busch, A.E., Steinmeyer, K., 2000. Molecular cloning and functional expression of KCNQ5, a potassium channel subunit that may contribute to neuronal M-current diversity. J. Biol. Chem. 275, 22395–22400.

Marcotti, W., Kros, C.J., 1999. Developmental expression of the potassium current $I_{K,n}$ contributes to maturation of mouse outer hair cells. J. Physiol. 520, 653–660.

Marcotti, W., Johnson, S.L., Holley, M.C., Kros, C.J., 2003. Developmental change in the expression of potassium currents of embryonic, neonatal and mature mouse inner hair cells. J. Physiol. 548.2, 383–400.

Marres, H., van Ewijk, M., Huygen, P., Kunst, H., van Camp, G., Coucke, P., Willems, P., Cremers, C., 1997. Inherited nonsyndromic hearing loss. An audiovestibular study in a large family with autosomal dominant progressive hearing loss related to DFNA2. Arch. Otolaryngol. Head Neck Surg. 123, 573–577.

Nakagawa, T., Kakehata, S., Yamamoto, T., Akaike, N., Komune, S., Uemura, T., 1994. Ionic properties of I_K, n in outer hair cells of guinea pig cochlea. Brain Res. 661, 293–297.

Nouvian, R., Ruel, J., Wang, J., Guitton, M.J., Pujol, R., Puel, J.L., 2003. Degeneration of sensory outer hair cells following pharmacological blockade of cochlear KCNQ channels in the adult guinea pig. Eur. J. Neurosci. 17, 2553–2562.

Oliver, D., Knipper, M., Derst, C., Fakler, B., 2003. Resting potential and submembrane calcium concentration is inner hair cells in the isolated mouse cochlea are set by KCNQ-type potassium channels. J. Neurosci. 23, 2141–2149.

Ryan, A., Dallos, P., 1975. Effect of absence of cochlear outer hair cells on behavioural auditory threshold. Nature 253, 44–46.

Schroeder, B.C., Hechenberger, M., Weinreich, F., Kubisch, C., Jentsch, T.J., 2000. KCNQ5, a novel potassium channel broadly expressed in brain, mediates M-type currents. J. Biol. Chem. 275, 24089–24095.

Talebizadeh, Z., Kelley, P.M., Askew, J.W., Beisel, K.W., Smith, S.D., 1999. Novel mutation in the KCNQ4 gene in a large kindred with dominant progressive hearing loss. Hum. Mutat. 14, 493–501.

Van Camp, G., Coucke, P.J., Akita, J., Fransen, E., Abe, S., De Leenheer, E.M., Huygen, P.L., Cremers, C.W., Usami, S., 2002. A mutational hot spot in the KCNQ4 gene responsible for autosomal dominant hearing impairment. Hum. Mutat. 20, 15–19.

Van Hauwe, P., Coucke, P.J., Ensink, R.J., Huygen, P., Cremers, C.W., Van Camp, G., 2000. Mutations in the KCNQ4 K+ channel gene, responsible for autosomal dominant hearing loss, cluster in the channel pore region. Am. J. Med. Genet. 93, 184–187.

Wang, H.S., Pan, Z., Shi, W., Brown, B.S., Wymore, R.S., Cohen, I.S., Dixon, J.E., McKinnon, D., 1998. KCNQ2 and KCNQ3 potassium channel subunits: molecular correlates of the M-channel. Science 282, 1890–1893.

Yang, S.M., Jing, S., Doi, T., Kaneko, T., Yamashita, T., 2002. Isolation of guinea pig inner hair cells using manual microsurgical dissection. J. Oto-Rhino-Laryngol. 64, 1–5.

Zhang, Z., Zeng, X.H., Xia, X.M., Lingle, C.J., 2009. N-terminal inactivation domains of beta subunits are protected from trypsin digestion by binding within the antechamber of BK channels. J. Gen. Physiol. 133, 263–282.

Effect of hydrogen peroxide on potassium currents in inner hair cells isolated from guinea pig cochlea

Takashi Kimitsuki, Noritaka Komune, Teppei Noda, Kazutaka Takaiwa, Mitsuru Ohashi and Shizuo Komune

Hydrogen peroxide (H_2O_2) is a ubiquitous reactive oxygen species that can induce several inner ear disorders. In this study, we recorded the potassium (K) currents in acutely isolated inner hair cells of guinea pig cochlea, and investigated the effects of H_2O_2. We also observed the morphological changes in inner hair cells induced by H_2O_2. In the H_2O_2 solutions, the amplitude of outward K currents ($I_{K,f}$ and $I_{K,s}$) clearly decreased after perfusion for approximately 15 min. Despite the decrease in outward currents, small inward currents ($I_{K,n}$) did not show any reduction. H_2O_2 induced morphological changes in the inner hair cells. All the inner hair cells in the H_2O_2 solutions showed shrinkage and granularity of the cell body and led to loss of viability. These results showed the vulnerability of inner hair cells to reactive oxygen species-induced inner ear disorders. *NeuroReport* **21:1045–1049 © 2010 Wolters Kluwer Health | Lippincott Williams & Wilkins.**

NeuroReport 2010, 21:1045–1049

Keywords: inner ear, ion current, morphology, organ of corti, reactive oxygen species

Department of Otolaryngology, Graduate School of Medical Sciences, Faculty of Medicine, Kyushu University, Fukuoka, Japan

Correspondence to Dr Takashi Kimitsuki, Department of Otolaryngology, Graduate School of Medical Sciences, Faculty of Medicine, Kyushu University, 3-1-1 Maidashi, Higashi-ku, Fukuoka 812-8582, Japan
Tel: +81 92 642 5668; fax: +81 92 642 5685;
e-mail: kimitaka@qent.med.kyushu-u.ac.jp

Received 12 July 2010 accepted 23 August 2010

Introduction

Reactive oxygen species (ROS) have been postulated to be involved in disorders of the inner ear, such as ischemic impairment [1], presbycusis [2], acoustic trauma [3], and labyrinthitis [4]. ROS are also involved in drug-induced hearing impairment. Gentamicin, an aminoglycoside antibiotic, produced ROS, and free radicals were detected in auditory hair cells after gentamicin treatment [5]. Cisplatin damages hair cells by lowering the antioxidant defense system of the inner ear [6]. In humans, the production of superoxide in inner ear perilymph has recently been reported in profound hearing loss [7].

Hydrogen peroxide (H_2O_2) is a ubiquitous ROS that can easily penetrate the cell membranes and is converted to the hydroxyl radical in the presence of Fe^{2+}. In addition to the transition of hydroxyl radical formation, an intracellular Ca^{2+} was elevated [8], which has been suggested to be involved in H_2O_2 toxicity [9]. H_2O_2-induced morphological changes, including bleb formation at the synaptic pole and shortening of the major axis of the cells has been observed in both cochlear hair cells [10,11] and vestibular hair cells [12].

In the mammalian cochlea, inner hair cells receive nearly all the afferent innervations and are primary acoustic transducers. Several ion channels are involved in the inner hair cell function, that is, receiving the mechanical displacement of stereocilia on the apical surface of the cells generates transmitter release onto auditory nerve endings at the basal pole of the cells. The potassium (K) currents are largest and possess the most robust properties compared with other ion currents, such as mechanoelectrical transducer currents and voltage-gated Ca^{2+} currents. Potassium currents, which determine the resting membrane potentials and allow the cells to perform high-frequency transduction by shortening the membrane time constant [13], are crucial for maintaining the cell physiological functions.

In this study, we isolated the inner hair cell from guinea pig cochlea and identified K currents to evaluate the influence of H_2O_2 on membrane ion channels in inner hair cells. The morphological changes in the inner hair cells by H_2O_2 were also investigated.

Materials and methods

Adult albino guinea pigs (200–350 g) with normal Preyer reflex were killed by rapid cervical dislocation, both bullae were removed and the cochlea was exposed. The cochlea, fused to the bulla, was placed in a Ca^{2+}-free external solution (in mM: 142 NaCl, 4 KCl, 3 $MgCl_2$, 2 NaH_2PO_4, 8 Na_2HPO_4, adjusted to pH 7.4 with NaOH). The otic capsule was opened, allowing removal of the organ of Corti attached to the modiolus. The organ of Corti was treated with trypsin (0.5 mg/ml, T-4665; Sigma-Aldrich, Missouri, USA) for 12 min, and gentle mechanical trituration was carried out. Trypsin was rinsed from the specimen by perfusing with a standard external solution (in mM: 142 NaCl, 4 KCl, 2 $MgCl_2$, 1 $CaCl_2$, 2 NaH_2PO_4, 8 Na_2HPO_4, adjusted to pH 7.4 with NaOH) for at least 10 min before starting any experiment.

0959-4965 © 2010 Wolters Kluwer Health | Lippincott Williams & Wilkins

DOI: 10.1097/WNR.0b013e32833fcb56

The most important landmarks for identifying inner hair cells are a tight neck and the angle between the cuticular plate and the axis of the cell.

Membrane currents were measured by conventional whole-cell voltage-clamp recordings using an EPC-10 (HEKA, Lambrecht, Germany). Data acquisition was controlled by the software PatchMaster (HEKA). Recording electrodes were pulled with a two-stage vertical puller (PP830, Narishige, Tokyo, Japan) using a borosilicate glass of an outer diameter of 1.5 mm (GC-1.5, Narishige, Tokyo, Japan) filled with an internal solution (in mM: 144 KCl; 2 $MgCl_2$; 1 NaH_2PO_4; 8 Na_2HPO_4; 2 ATP; 3 D-glucose; 0.5 EGTA; adjusted to pH 7.4 with KOH). Pipettes showed a resistance of 4–8 MΩ in the bath and were coated with ski wax (Tour-DIA, DIAWax, Otaru, Japan) to minimize capacitance. The capacitance of the cell was 11.3 ± 3.2 pF [mean ± standard deviation (SD)] and the series resistance was 16.3 ± 5.4 MΩ ($n = 19$). Hydrogen peroxide (H_2O_2, H1009, Merck, Darmstadt, Germany) was applied under pressure (Pressure micro-injector: PMI-200, Dagan, Minneapolis) using pipettes with a tip diameter of 2–4 μm positioned approximately 50 μm from the inner hair cells. These cells were continuously perfused with external saline and all experiments were performed at room temperature (20–25°C).

Isolated inner hair cells were observed under an inverted microscope (TE2000-U, Nikon, Tokyo, Japan) using a CCD video camera (Sony, XC-ST70/ST70CE, Tokyo, Japan) and images were captured into the video frames (Sony DCR HC62).

The experimental design was reviewed and approved (accession number: A21-085-0) by the Animal Care and Use Committee, Kyushu University. All procedures were conducted in accordance with the Guidelines for Animal Care and Use Committee, Kyushu University.

Results

Membrane currents in response to hyperpolarizing and depolarizing voltage steps from a holding potential of −60 mV were recorded from inner hair cells. Typical current records in standard solutions are shown in Fig. 1a. Inner hair cells showed outwardly rectifying K currents ($I_{K,f}$ and $I_{K,s}$) in response to depolarizing voltage pulses, with only a slight inward current ($I_{K,n}$) when hyperpolarized. After 15 min, the K currents did not show noticeable changes in either amplitude or shape (Fig. 1a in right panel). In the solution of 10 mM H_2O_2, the amplitude of K current decreased after perfusion for 15 min (Fig. 1b). Despite the decrease in outward currents, small inward currents did not show any reduction. The activating kinetics in each voltage-dependent outward K current preserved a fast rising rate (lower enlarged scale in Fig. 1b).

Morphological changes in inner hair cells were observed after the application of 10 mM H_2O_2 with the depression of K currents (Fig. 2). H_2O_2 induced shrinkage and granularity of the cell body after approximately 10 min and led to loss of viability. All four inner hair cells were unable to survive in 10 mM H_2O_2 solutions for 20 min.

A comparison of the amplitude of outward K currents recorded in control solutions and 10 mM H_2O_2 solutions is shown in Fig. 3. The amplitudes of outward K currents at +110 mV were measured after the application of standard or H_2O_2 solutions for 5, 10, and 15 min and amplitudes relative to those at 0 min were shown from 15 inner hair cells in control and four inner hair cells in H_2O_2 solutions. Five minutes after application, mean ± SDs were 0.97 ± 0.16 and 0.76 ± 0.09 for control and H_2O_2 solutions, respectively, showing a significant difference ($P < 0.05$). After 10 min, mean ± SDs were 0.91 ± 0.14 and 0.66 ± 0.10 for control and H_2O_2 solutions, respectively, showing a significant difference ($P < 0.05$). After 15 min, mean ± SDs were 0.90 ± 0.09 and 0.45 ± 0.12 for control and H_2O_2 solutions, respectively, also showing a significant difference ($P < 0.01$).

Discussion

The effects of H_2O_2 on the K channels in cochlear inner hair cells were studied. H_2O_2 inhibited channel activity and decreased the current amplitudes within 15 min. There was no change in the activating kinetics of the channel (Fig. 1b). H_2O_2 by itself is not sufficiently reactive to oxidize organic molecules in an aqueous environment. Nevertheless, H_2O_2 has the ability to generate highly reactive hydroxyl-free radicals through its interaction with redox-active transitional metals (Fe^{2+} or Cu^{+}, 'Fenton reaction'). Hydroxyl-free radicals oxidize cell membrane lipids and alter cell membrane enzymes and receptors, leading to changes in membrane permeability and the ionic gradient [14]. Although H_2O_2 is a physiologically ubiquitous ROS, an excess production of superoxide in human perilymph of the inner ear with profound hearing loss was established by spectrophotometric analyses [7].

In addition to the 'Fenton reaction' an increase in the cytosolic Ca^{2+} concentration $[Ca^{2+}]_i$ has been suggested to be involved in H_2O_2 toxicity [9]. H_2O_2-induced $[Ca^{2+}]_i$ elevation was reported to be in a concentration-dependent manner [8]. Protection by the calcium channel blocker, nifedipine, of the H_2O_2-induced outer hair cell death [11], suggests the participation of voltage-gated Ca^{2+} channels in H_2O_2-induced $[Ca^{2+}]_i$ elevation. An increase of cytosolic calcium has been shown to be involved in the intracellular Ca^{2+} stores [9], which was independent of voltage-gated Ca^{2+} channels [15]. The reduction of K channel activity in this study showed a voltage-independent behavior (Fig. 1b), suggesting the contribution of Ca^{2+} stores. A rise of $[Ca^{2+}]_i$ has been associated with cytotoxic effects, such as destruction of the cytoskeleton, membrane injury, DNA fragmentation,

Fig. 1

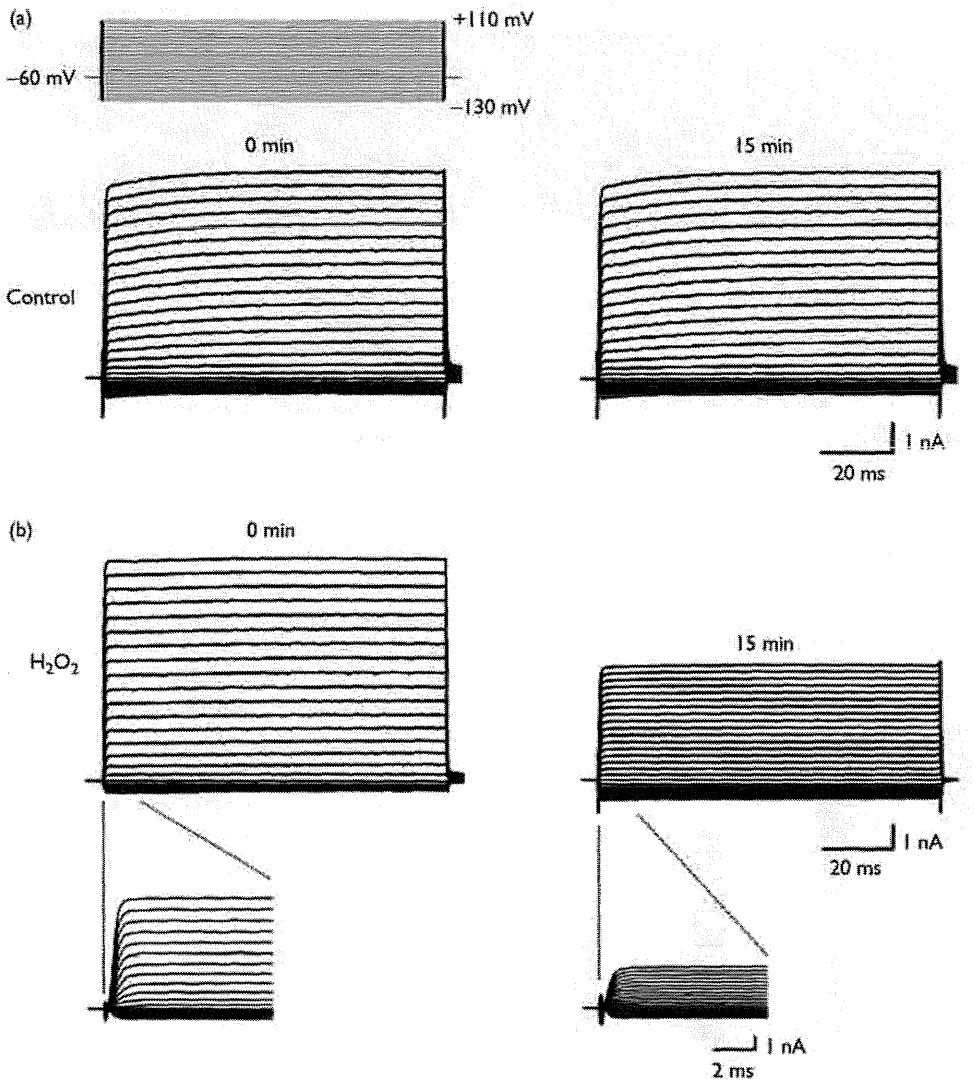

Effects of hydrogen peroxide (H_2O_2) on potassium (K) currents in inner hair cells. (a) K currents in control solutions at 0 and 15 min. The upper panel shows the voltage step protocol. (b) K currents in 10 mM H_2O_2 solutions at 0 and 15 min after application. The lower insets show the initial activating phase in expanded time scales.

and damage to cell organelles such as mitochondria [16]. Exposure of the cells to H_2O_2 results in an increased formation of oxidized protein sulfhydryl groups. The redox state of protein sulfhydryl groups also affects Ca^{2+} homeostasis [17]. Antioxidants, such as glutathione and N-acetylcysteine, suppressed the continuous increase of cytosolic Ca^{2+} and protected against H_2O_2-induced cell damage [18].

Oxidative stress is related to swelling of the cell body, bleb formation, and shortening of the neck region in vestibular hair cells [12], formation of cytoplasmic blebs at the infranuclear pole, and the diminution of outer hair cells [10]. These morphological changes were concentration-dependent. Although a concentration of 10 mM H_2O_2 is sufficient to produce the morphological changes in the cells, inner hair cells in this study did not show any bleb formations or shortening of the cells, but showed shrinkage and granularity of the cell body. Bleb formation in the cell membrane is considered as the response to altered membrane integrity in the absence of cytoskeletal support elements [10,12]. The cortical lattice is one of the cytoskeletal support elements and has a network of actin filaments with colocation of spectrin [19]. Gamma-actin was particularly associated with the lateral wall of the outer and inner hair cells, but became sparse in areas in which the cortical lattice terminates below the region of the nucleus [20]. The amount and distribution of the cortical lattice are different between the outer and inner hair cells [21], so the alteration of the membrane

Fig. 2

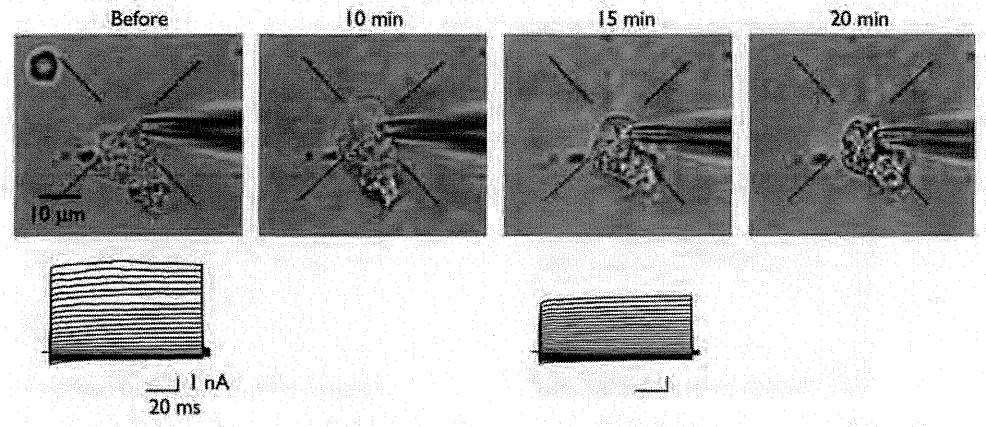

Morphological changes of inner hair cells after the application of 10 mM hydrogen peroxide (H_2O_2). The lower records show the potassium currents before and 15 min after the H_2O_2 application. H_2O_2 induced shrinkage and granularity of the cell body.

Fig. 3

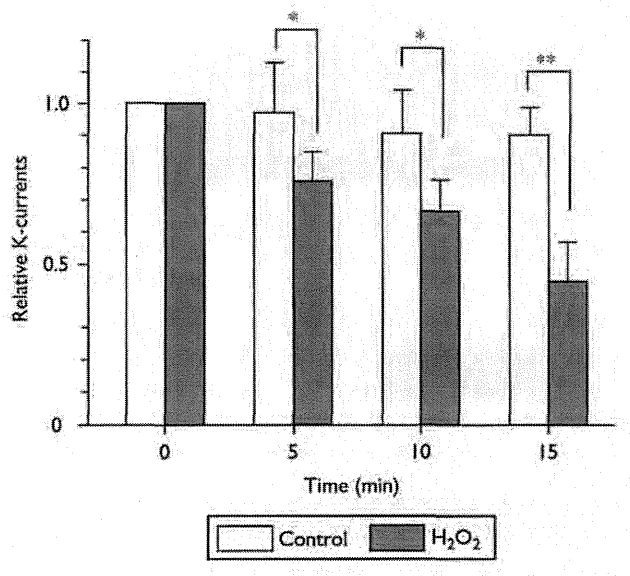

Comparison of the amplitude change in outward potassium (K) currents between control and 10 mM hydrogen peroxide solutions. Test pulse voltage was +110 mV. *$P<0.05$, **$P<0.01$.

integrity by H_2O_2 might also be different, causing differences in the pattern of morphological changes between the outer and inner hair cells.

In the inner hair cells, three types of potassium currents ($I_{k,f}$, $I_{k,s}$, and $I_{k,n}$) were distinguishable [13]. The fast-activating current, $I_{k,f}$, was blocked by tetraethylammonium but was resistant to 4-aminopyridine. The properties of $I_{k,f}$ in the inner hair cells resemble the Ca^{2+}-activated K^+ [big potassium (K), BK] currents because of their kinetics and pharmacology [22], and the K^+ currents in the inner hair cells are potentiated by increasing intracellular Ca^{2+} [23]. Ca^{2+}-activated K^+ channels expressed in *Xenopus* oocytes were inhibited by oxidation with H_2O_2 [24,25]. They reported that H_2O_2 decreased both the open channel probability and the number of active channels based on noise analysis of macroscopic currents. H_2O_2 did not affect channel activity when added to the extracellular side, providing evidence for an intracellular site of H_2O_2 action [24]. H_2O_2 also accelerated the rate of channel 'run-down' [25]. In this study, the channel activity inhibited by H_2O_2 was time-dependent (Fig. 3), which might represent the time course of H_2O_2 uptake into the cell or represent the process of K channel 'run-down'.

Conclusion

In cochlear inner hair cells, H_2O_2, a ubiquitous ROS, inhibited the activation of outward K currents after perfusion of approximately 15 min. H_2O_2 induced acute morphological changes in inner hair cells such as shrinkage and granularity of the cell body, leading to loss of viability. Inner ear disorders involving ROS could be initially elicited by functional and morphological changes in the inner hair cell.

Acknowledgement

This study was supported by a Grant-in-Aid for Scientific Research 21592160 from the Ministry of Education, Culture, Sports, Science and Technology of Japan.

References

1 Maetani T, Hakuba N, Taniguchi M, Hyodo J, Shimizu Y, Gyo K. Free radical scavenger protects against inner hair cell loss after cochlear ischemia. *Neuroreport* 2003; **14**:1881–1884.
2 Staecker H, Zheng QY, Van de Water TR. Oxidative stress in aging in the C57B16/J mouse cochlea. *Acta Otolaryngol* 2001; **121**:666–672.
3 Yamasoba T, Schacht J, Shoji F, Miller JM. Attenuation of cochlear damage from noise trauma by an iron chelator, a free radical scavenger and glial cell line-derived neurotrophic factor in vivo. *Brain Res* 1999; **815**:317–325.

4 Takumida M, Popa R, Anniko M. Lipopolysaccharide-induced expression of reactive oxygen species and peroxynitrite in the guinea pig vestibular organ. *ORL J Otorhinolaryngol Relat Spec* 1998; **60**:254–262.
5 Hirose K, Hockenbery DM, Rubel EW. Reactive oxygen species in chick hair cells after gentamicin exposure *in vitro*. *Hear Res* 1997; **104**:1–14.
6 Lautermann J, Crann SA, McLaren J, Schacht J. Glutathione-dependent antioxidant systems in the mammalian inner ear: effects of aging, ototoxic drugs and noise. *Hear Res* 1997; **114**:75–82.
7 Ciorba A, Gasparini P, Chicca M, Pinamonti S, Martini A. Reactive oxygen species in human inner ear perilymph. *Acta Otolaryngol* 2010; **130**:240–246.
8 Ishii M, Shimizu S, Hara Y, Hagiwara T, Miyazaki A, Mori Y, *et al.* Intracellular-produced hydroxyl radical mediates H_2O_2-induced Ca^{2+} influx and cell death in rat beta-cell line RIN-5F. *Cell Calcium* 2006; **39**:487–494.
9 Hyslop PA, Hinshaw DB, Schraufstatter IU, Sklar LA, Spragg RG, Cochrane CG. Intracellular calcium homeostasis during hydrogen peroxide injury to cultured P388D1 cells. *J Cell Physiol* 1986; **129**:356–366.
10 Clerici WJ, DiMartino DL, Prasad MR. Direct effects of reactive oxygen species on cochlear outer hair cell shape *in vitro*. *Hear Res* 1995; **84**:30–40.
11 Dehne N, Lautermann J, Ten Cate WJ, Rauen U, De Groot H. *In vitro* effects of hydrogen peroxide on the cochlear neurosensory epithelium of the guinea pig. *Hear Res* 2000; **143**:162–170.
12 Tanigawa T, Tanaka H, Hayashi K, Nakayama M, Iwasaki S, Banno S, *et al.* Effects of hydrogen peroxide on vestibular hair cells in the guinea pig: importance of cell membrane impairment preceding cell death. *Acta Otolaryngol* 2008; **128**:1196–1202.
13 Kros CJ, Crawford AC. Potassium currents in inner hair cells isolated from the guinea-pig cochlea. *J Physiol* 1990; **421**:263–291.
14 Halliwell B. Reactive oxygen species and the central nervous system. *J Neurochem* 1992; **59**:1609–1623.
15 Kimura M, Maeda K, Hayashi S. Cytosolic calcium increase in coronary endothelial cells after H_2O_2 exposure and the inhibitory effect of U78517F. *Br J Pharmacol* 1992; **107**:488–493.
16 Orrenius S, McConkey DJ, Bellomo G, Nicotera P. Role of Ca^{2+} in toxic cell killing. *Trends Pharmacol Sci* 1989; **10**:281–285.
17 Bellomo G, Orrenius S. Altered thiol and calcium homeostasis in oxidative hepatocellular injury. *Hepatology* 1985; **5**:876–882.
18 Lomonosova EE, Kirsch M, De Groot H. Calcium vs. iron-mediated processes in hydrogen peroxide toxicity to L929 cells: effects of glucose. *Free Radic Biol Med* 1998; **25**:493–503.
19 Slepecky NB, Ulfendahl M. Actin-binding and microtubule-associated proteins in the organ of Corti. *Hear Res* 1992; **57**:201–215.
20 Furness DN, Katori Y, Mahendrasingam S, Hackney CM. Differential distribution of beta- and gamma-actin in guinea-pig cochlear sensory and supporting cells. *Hear Res* 2005; **207**:22–34.
21 Furness DN, Hackney CM. Comparative ultrastructure of subsurface cisternae in inner and outer hair cells of the guinea pig cochlea. *Eur Arch Otorhinolaryngol* 1990; **247**:12–15.
22 Art JJ, Fettiplace R. Variation of membrane properties in hair cells isolated from the turtle cochlea. *J Physiol* 1987; **385**:207–242.
23 Dulon D, Sugasawa M, Blanchet C, Erostegui C. Direct measurement of Ca^{2+}-activated K^+ currents in inner hair cells of the guinea-pig cochlea using photolable Ca^{2+} chelators. *Pflüg Arch* 1995; **430**:365–373.
24 Soto MA, González C, Lissi E, Vergara C, Latorre R. Ca^{2+}-activated K^+ channel inhibition by reactive oxygen species. *Am J Physiol Cell Physiol* 2002; **282**:C461–C471.
25 DiChiara TJ, Reinhart PH. Redox modulation of hslo Ca^{2+}-activated K^+ channels. *J Neurosci* 1997; **17**:4942–4955.

JOHNS
特集●伝音難聴の耳よりな話●

一側性耳硬化症は手術するのか？

熊川孝三*
Kozo KUMAKAWA

● Key Words ●一側性耳硬化症，アブミ骨手術，適応基準●

はじめに

耳硬化症は白色人種では人口の0.5％に発症するが，黄色人種や黒色人種には少なく，日本人での頻度は1万人に1人であると言われている。80～85％が両側同時か，または前後して両側性に発症し，真の一側性耳硬化症は少ない。

一側性の耳硬化症患者は，術後に必然的に正常側との比較を行う。さらに一時的にではあっても，味覚障害やめまいを伴うことを考えると，手術適応としない施設もあることは十分に理解可能である。本稿では，手術適応と手術を成功させるためのポイントを中心に述べる。

I．一側性耳硬化症の定義

次の3つの病態に当てはまるものが，臨床的には“一側性耳硬化症”といえよう。

1）真の一側性耳硬化症（ここでは患側が40 dB以上でアブミ骨筋検査が陰性，健側が25 dB未満でアブミ骨筋検査が陽性なものと定義する）
2）両側性であるが，一側は初期で正常範囲内
3）両側性であったが，一側は手術により正常レベルにまで改善

最近はドックでの聴力検査や診断技術の向上で発見は増加傾向にあり，また手術を行う施設数も増えており，これに伴って一側性の例も必然的に増加傾向がある。ちなみに当院での最近3年間の耳硬化症に対するアブミ骨手術件数は106例であったが，内訳は1）が17例16％，2）が7例6.6％，3）が9例8.5％，そして両側性が73例68.9％であった。すなわち，真の一側性耳硬化は16％であったが，聴覚的な“一側性耳硬化症”は31.1％であり，臨床的には重要である。

II．当院の一側性耳硬化症の手術適応基準

以下の項目のうち，3項目以上に該当し，かつ本人の希望があれば当科ではアブミ骨手術の適応としている。

1）標準純音聴力検査の会話域で気導値と骨導値の差が30 dB以上ある。
2）語音聴力検査で患側が伝音難聴パターンを示し，かつ50～60 dBの検査音で聴取成績の低下がある。
3）主に電話を使用する側が患側であり，社会生活上の問題がある
4）音の方向感が低下している。
5）騒音下での聞き取り能力が低下している。

1）の理由は，低音域のみが低下し，高音域が正常に近い，いわゆるstiffness curveを呈する一側性例では，まだ固着程度が軽く，底板が前庭へ落ち込むfloating footplateの合併症を生じやすいためである。

2）は，その音圧が普通会話音レベルに相当し，その低下は患側からの会話聴取に影響を与えるからである。

3）は，例えば左が患側であり，右で電話を聞くが，同時に右手でメモを取るため不自由な場合などが該当する。

4），5）については，Holら[1]は，一側性伝音難聴（会話域の平均聴力レベルが53 dBの一側性伝音難聴13症例）に方向感検査を施行し，両側の気

* 虎の門病院耳鼻咽喉科・聴覚センター
〔〒105-8470 東京都港区虎ノ門2-2-2〕

導値差が40 dB以上の症例では方向感が低下したと報告している。

また，彼らは同じ患者群に自由音場での正面からの語音了解閾値検査speech recognition threshold test（SRT，50％の語音了解度を示す語音聴力レベルを求める検査）も行った結果，両側正常群では静寂時でもSRT値が20 dBであるのに対して，これらの一側性伝音難聴患者群では静寂時のSRT値が26.8～42.0 dB（平均32 dB）となり，両側正常群より12 dB上昇したと述べている。

さらに健側側面から65dBSPLの騒音負荷を与えた場合は，静寂時に比べて，約30 dBのSRT値上昇が生ずることを報告した。すなわち，一側性伝音難聴患者も静寂時に音場での語音聴取能が低下するが，軽度であるために気付きにくい。ただし，騒音負荷時には気付きやすくなることが推測される。

これを実際に患者に体験させるには，図1のような検査方法で，数字を用いた音場での静寂時と騒音負荷時SRT検査を行う。騒音負荷時のSRT値の悪化によって，患者も自身の片耳難聴に伴う問題点を把握でき，手術に踏み切るべきか否かの判断に役立つ。

当科では，以上の問題をよく理解し，さらに次の手術説明に同意された患者だけを手術適応としている。

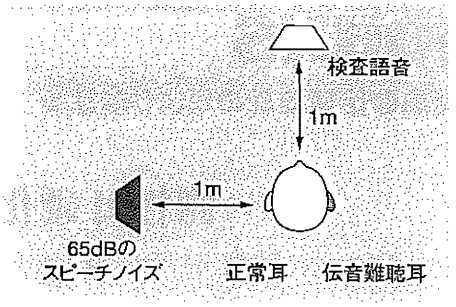

図1　自由音場での騒音負荷による語音検査方法

Ⅲ．手術同意のための説明文書

一側性では，患者は術後に必然的に正常聴力側との比較を行うため，わずかな差があっても悩む。また，耳鳴りについてもこれらが術後に消失しないことを問題視しがちである。したがって，術前に十分な説明を文書で行い，同意を得た上で手術を行う。参考に当院での説明文書の一部を掲載する。

「手術を行った方には，次のような問題を起こす可能性があります」

1）手術側の舌の味覚が一時的に変わったりするかもしれません。

2）アブミ骨に穴を開けることで，めまいが起こります。その期間は3～4日位と考えられますが，個人差があります。

3）耳鳴りの一時的な増強が起こるかもしれません。また，手術前から存在した耳鳴りは内耳で起こっているもので，原則的に手術では改善されません。ただし，30％～40％位の方では改善も認められます。聞こえが良くなったことで耳鳴りが気にならなくなるという方もいます。

4）200～300例に1例の割合で，内耳と脳周囲のクモ膜下腔の間に，奇形的なミクロの連絡通路が存在している場合があります。この場合には，手術でアブミ骨底板に小穴を開けた際に，外リンパ液が流れ出る現象が合併症として発生し，これを塞ぐために人工アブミ骨を入れることができなくなり，聴力の改善が難しい，あるいは時に悪化することがありえます。

5）人工の骨を使いますから，将来，何らかの拒絶反応を起こす可能性もあります。

6）人工の骨で手術した側の聴力が，神様が創ってくれた自然の耳とまったく同じになるわけではありません。正常耳との比較ではなく，手術前の聴力との比較をするように心がけて下さい。

Ⅳ．手術を確実に成功させるためのポイント

一側性では侵襲を最小限に行うことが，両側性の場合以上に要求される。

1．麻酔の選択

ラリンジアルマスクによる全身麻酔下に行う。

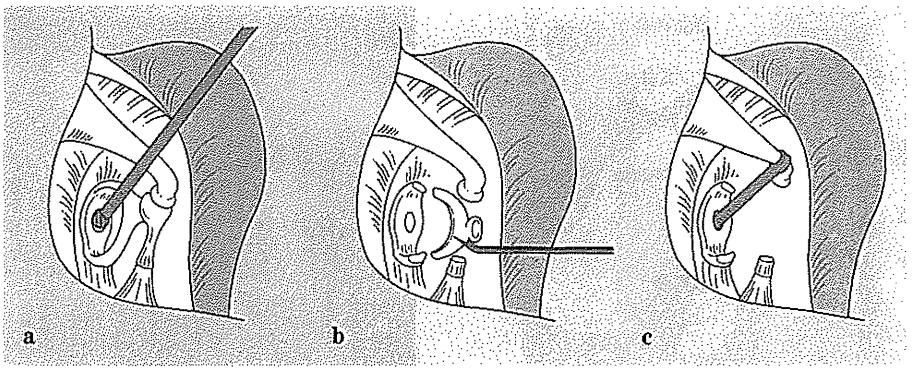

図 2　著者の小開窓アブミ骨手術の手順
a：良好な視野で先にアブミ骨底小開窓を行う。b：キヌタ・アブミ関節離断とアブミ骨上部構造摘出。c：テフロンピストン挿入

その利点として，抜管時のバッキングがなく，外リンパの漏出やピストン脱落の不安も少ない。術後の咽頭痛・嗄声も軽度である[2]。

2．外耳道切開・削開方法

当科では，ほぼ全例を経外耳道法で行う。耳後法よりも角度的にアブミ骨底を見やすい。ポイントは狭い外耳道では高い外耳道輪状切開で行うことである。鼓索神経の切断はもちろん，引き伸ばしもいけない。そのままの位置で行うことが肝要である。

3．小開窓アブミ骨手術

アブミ骨底全体を除去する total stapedectomy (TS) とアブミ骨底に小開窓を行う small fenestra stapedectomy (SFS) があるが，術後成績，術後のめまいが少ない，血管膜や筋膜などを採取する必要もない，などの利点から可及的に SFS を行う。

日本人の耳硬化症では，アブミ骨底が薄く，また固着程度が軽く，SFS を意図してもアブミ骨脚の切断や底の開窓に伴い，底板が割れたり，可動状態となり，結果的に TS にせざるをえない例が意外に多いことが報告されている。これを避ける方法として，

1）アブミ骨脚の切断方法

過去にはアブミ骨剪刀の使用していたが，予想以上の力を要し，底板が可動となってしまう例があり，現在は使用していない。低回転電気ドリルあるいはレーザーによる切断を勧める。後脚のみでなく，見えれば前脚も切断し，アブミ骨脚の骨折操作を可及的に避けることが望ましい。

2）良好な視野では先にアブミ骨底小開窓を

特にアブミ骨底の固着が軽く，前述の懸念が予測される例では，図 2 のように，アブミ骨がキヌタ骨にしっかりと固定されている状態で先に小開窓する。その後，アブミ骨筋切断，IS 関節離断，脚切断，ピストン挿入という手順でゆく。したがって safety hole は設けない。この利点は，万が一，この後のアブミ骨脚切断操作などで底板が可動となっても，SFS の術式が続行可能なところにある。ただしこの手技が可能なのは顔面神経の下垂がなく，かつアブミ骨後脚によってアブミ骨底が隠されていない例（約 3/4 の症例）に限られる。見えない例では，通常通り，まずアブミ骨筋切断，IS 関節離断，脚切断，そして小開窓という手順でゆく。

Fish[3]が提唱したように，先に開窓後，直ちにピストン挿入を先行して，後で IS 関節離断とアブミ骨上部構造摘出を行うという，ピストン挿入先行 SFS もある。外リンパの漏出や血液の流入の危険性も少なく，術後のめまいや嘔吐がこれまでの方法に比べてはるかに軽度であった[4]。ただし，ピストン装着後の狭い部位での複雑な操作は，習熟していないと逆に難しい。

アブミ骨底の小開窓には手もみドリルではな

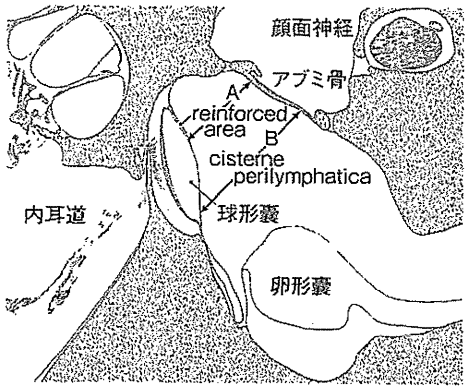

図 3　アブミ骨底板と球形嚢の関係（5より引用）
底板前方（A）では後方（B）より球形嚢までの距離が短いため，底板後方での開窓がより安全である。

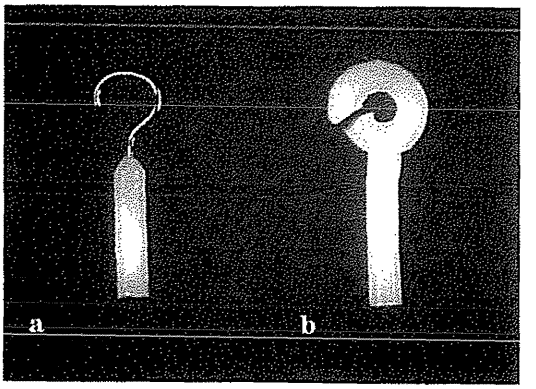

図 4　テフロンワイヤーピストン（a）とテフロンピストン（b）

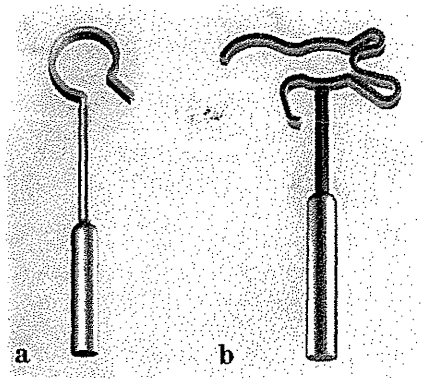

図 5　最新の KURZ 社チタン製ピストン
a：K-piston，b：Soft Clip Piston

く，専用機器を容易すべきである。これにはステーピースハンドピース（GYRUS 社製 Diego Dissector System），スキータードリル（Medtronic XOMED 社製 XPS3000 System）などの低回転電気ドリルあるいはレーザーなどがあるが，底板の厚い例，海綿状骨増殖がある例ではレーザーのみでは難渋し，ドリルの方が容易である。開窓は使用ピストンの直径＋0.2 mm のドリルを選択する。

10 年以上の長期の経過観察結果から，少し大きめの開窓の方が良好な聴力を維持できると考える。年齢を考慮して開窓サイズを決めるのも一法である。

3）底板開窓部の位置

開窓位置は重要である。図 3 に示すように，前方を開けるのは，球形嚢が底板に近い可能性があり，危険である。中央あるいは後方，すなわち posterior half を開けることが望ましい。高名なアブミ骨術者である Causse も，ピストンによる内耳損傷を避けるためには posterior half stapedectomy が良いと述べている[6]。

4．ピストン選択

一般的にワイヤーピストン（図 4-a）が好まれて使用されている。ワイヤーピストンはそのステンレスの鋼種は SUS316 であり，これは非磁性である。このため MRI 検査でも動きの問題はないが，ワイヤーループに磁場の急激な変化で起電力が発生し，熱を帯びることが MRI メーカーによって確認されている。チタン製ピストンは軽量で高磁場 MRI 検査も可能であり，海外ではすでに認可を受けて従来のワイヤーピストンに代わるものとして使用されている。

著者は GYRUS 社のシャフト径 0.6 mm のテフロンピストン（図 4-b），あるいは最近開発されたシャフト径 0.4 mm の KURZ 社製チタン製ピストン K-piston や Soft Clip Piston（現在は個人輸入が必要，図 5）を使用している。直径が細いため，顔面神経下垂例では開窓も小さく済み，また顔面神経にもシャフトが触れないので有用である。

アブミ骨底からキヌタ骨までの距離＋0.5 mm が一般的である。

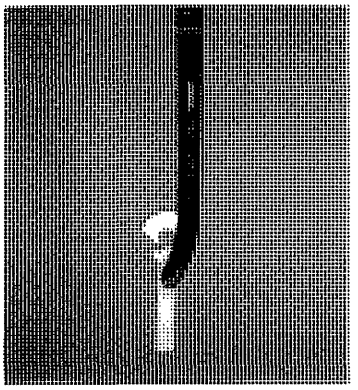

図 6　テフロンピストンのトリミングと保持方法

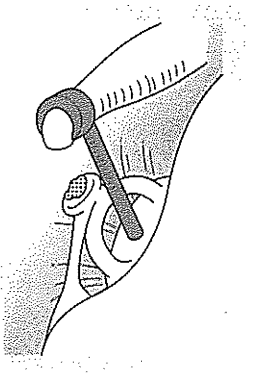

図 7　高木式アブミ骨保存小開窓アブミ骨手術

5．ピストンのトリミングと挿入

ワイヤーピストンに慣れた術者にとってピストンリングは扱いにくいという声があるが，リングは拡げただけでは入りにくい。図6のようにリングの上部をメスで楔状に切除し，キヌタ骨の前方への動きを左手のホルダーで抑え，ピストン先端を開窓部に入れた後に，リングの切除開大部分をキヌタ骨長脚に向かって前方に軽く押し込むことで容易に装着可能である。その後，リングは自然に締まる。筆者は自作のキヌタ骨長脚ホルダーとピストンリング専用横開き鉗子を用いている。

この挿入方法は前述の Soft Clip Piston でも同様であり，合理的な方法と考える。

高木ら[7]が提唱した，キヌタ骨豆状突起のみを切除し，アブミ骨をそのままに，ピストンを挿入するアブミ骨保存小開窓手術（図7）も画期的である。筆者も4例試みたが，アブミ骨脚を切断せずとも底板がよく見える例では可能である。ただし，全例には施行できないことと，アブミ骨が邪魔になり，ピストンリングを通常の位置よりもキヌタ骨体側へ移動して装着せざるを得ず，これが耳小骨による増幅効果に問題を生じないか，豆状骨突起のスペースが狭いので，ここが再び接着しないかという懸念が残り，長期の観察結果を待っている。

6．術後の外リンパ瘻の予防

最も大事な点はSFSだからこそ起こりうる，術後の外リンパ瘻の防止である。このために開窓部とピストンの周辺に血液塊[3]やジェルフォーム，筋膜小片を置くなどの予防処置を行う。特にアブミ骨底にリスが入った場合などは遅れて外リンパ瘻が生ずることが稀にあり，必ず予防処置を講じておくべきである。フィブリン糊は逆に固着によって聴力が改善しなかった他院の例があり，使用していない。

おわりに

耳硬化症の聴力改善の喜びは患者，術者ともに大きいが，狭小な視野の中で行う微細な手術であり，外リンパ漏やアブミ骨底板の陥入などの合併症によって悪化あるいは聴力を失う懸念さえある。一側性耳硬化症では術後に必然的に正常側との比較を行うので，特に注意が必要であり，患者の了解度，手術設備と器具，術者の経験と成績などを総合的に考慮して，慎重に決定すべきと考える。

文　献

1) Hol MKS, Snik AFM, Mylanus EAM：Does the bone-anchored hearing aid have a complementary effect on audiological and subjective outcomes in patients with unilateral conductive hearing loss? Audiology and Neurotology **10**：159-168, 2005.
2) 高橋優宏，熊川孝三，他：耳科手術におけるラリンジアルマスク（LMA ProSeal）の使用経験．耳鼻展望 **47**：49-52, 2004.
3) Fisch U：Stapedotomy versus stapedectomy. Am J

Otol 9：112-117, 1982.
4) 熊川孝三：耳硬化症．今日の治療指針 2000，902 頁，医学書院，東京，2000.
5) 野村恭也，原田雄彦，平出文久：耳石器．耳科学アトラス―形態と計測値―，第 3 版，177 頁，シュプリンガー・ジャパン社，東京，2008.
6) Causse JB, Causse JR, Wiet RJ：Complications of stapedectomies. American Journal of Otology 4：275-280, 1983.
7) 高木　明，河田恭孝，岡部静也，他：耳硬化症のアブミ骨上部構造保存アブミ骨手術．Otology Japan 14：450，2004.

*　　*　　*

JOHNS
特集●耳鼻咽喉科領域の新しい診療機器●

聴性脳幹インプラント

熊川孝三[1)] 武田英彦[1)] 射場 恵[1)] 熊谷文愛[1)]
Kozo KUMAKAWA Hidehiko TAKEDA Megumi IBA Fumiai KUMAGAI
中冨浩文[2)] 臼井雅昭[2)] 関 要次郎[3)] 内藤 泰[4)]
Hirofumi NAKATOMI Masaaki USUI Yojiro SEKI Yasushi NAITO

● Key Words ●聴性脳幹インプラント，蝸牛神経核，下丘●

はじめに

内耳よりさらに中枢の聴神経由来の高度感音難聴については人工内耳でも電気信号を脳幹の神経核に伝えることができない。このような聴神経由来の難聴の外科的治療法として，蝸牛神経核（延髄での聴覚ニューロンの中継核）の表面上に電極を置いて，これを直接に電気刺激して聴覚を取り戻す人工臓器が開発されている。これが聴性脳幹インプラント（auditory brainstem implant，以下ABIと略す）である。

Ⅰ．聴覚伝導路の機能解剖

聴覚伝導路の基本的走行を図1に示した。内耳の蝸牛で音は振動から電気的な信号に変換され，同側延髄の中継核である蝸牛神経核（cochlear nucleus：CN）に届く。ここから同側と対側の上オリーブ核に分かれて，外側網体を上行し，中脳の下丘（inferior colliculus：IC）にて中継され，内側膝状体を通って，皮質聴覚野に伝えられる。ここで，ABIはCN上に置かれる。ABIは左右いずれのCN上に設置されても伝導路が交叉し，両側側頭葉に信号が伝えられるので言語の優位半球については考慮しなくともよい。

Ⅱ．歴史と本装置のシステム

ABIはロスアンジェルスにあるHouse耳科学研究所の脳外科医Hitselbergerによって考案され，1979年に両側の聴神経腫瘍を有する神経線維腫症第2型(neurofibromatosis type 2，以下NF2)の患者に第1例目の埋め込み手術が行われた[1)]。その時期は同僚の耳鼻咽喉科医であるHouseが人工内耳を考案した時とほぼ同時期であり，人工内耳とABIは，埋め込む位置こそ違え，聴神経路を電極で刺激して聴覚を再獲得するという発想のもとに同じ施設で同時に生まれたことは興味深い。

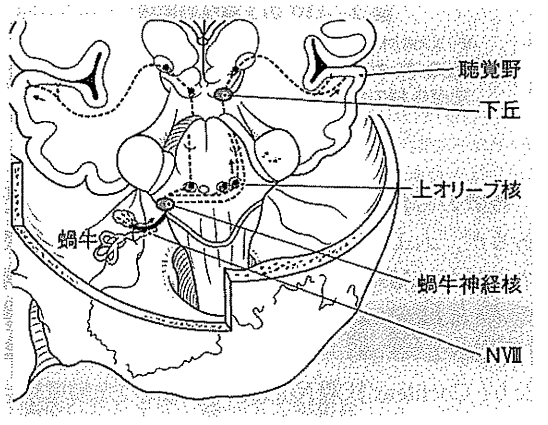

図1 聴覚伝導路の機能解剖

ABIは当初，単チャンネルであったが，その後，人工内耳の改良とともに多チャンネル化が図られた。現在，Cochlear社製Nuclues 24 ABI (24チャンネル)とMED-EL社製Pulser100 ABI (12チャンネル)の2種類がある。わが国では，まだ保険適用はなされていない。

[1)] 虎の門病院耳鼻咽喉科・聴覚センター，[2)] 同 脳神経外科〔〒105-8470 東京都港区虎ノ門2-2-2〕
[3)] 東京共済病院脳神経外科，[4)]神戸市立医療センター中央市民病院耳鼻咽喉科

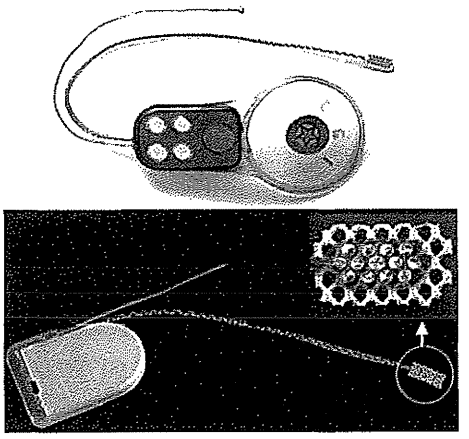

図 2　ABI の 2 種類の電極
a：Cochlear 社製 ABI 24 チャンネル。b：MED-EL 社製 ABI。12 チャンネル（挿入図は電極先端の拡大を示す）。

図 3　右側の蝸牛神経核とその付近の解剖
小脳を挙上し，第Ⅳ脳室底を斜め上から見る。DCN：蝸牛神経背側核，VCN：同腹側核，Ⅶ，Ⅷ，Ⅸ：各脳神経

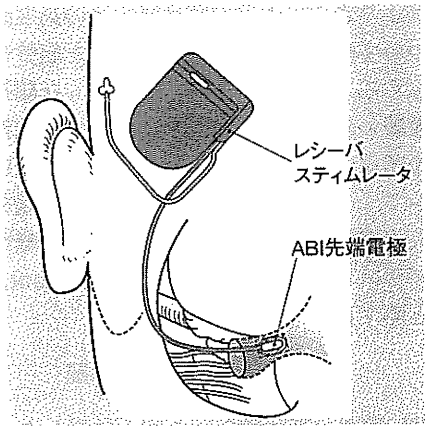

図 4　ABI 電極の設置
先端電極を外側陥凹 lateral recess の底部で蝸牛神経核上に置き，レシーバスティムレータを生体糊で固定する

装置のおおまかなシステムは人工内耳と同様であるが，人工内耳が内耳（蝸牛）に埋め込まれるのに対し，ABI はさらに中枢にある脳幹の蝸牛神経核 cochlear nucleus（CN）の表面に置かれる（図 1）。このため，人工内耳のリング状電極と異なり，Cochlear 社製 Nuclues 24ABI の先端電極は 3×8 mm の長方形で，ここに 22 個のディスク状電極が配列している。一方，MED-EL Pulser100 ABI の先端電極は 5.5×3.0 mm で 12 個の活性電極と 1 個の不活性電極が並んでいる（図 2）。

蝸牛神経核内においても神経細胞は周波数にしたがって tono-topical に配列しており，電極ごとのピッチ弁別が可能である。これを利用してフォルマント情報を伝える。体外システムは人工内耳と同様である。

Ⅲ．ABI の適応疾患

ABI の適応基準の対象例は両側の聴神経腫瘍の障害によって高度の難聴となる場合であり，ほとんどは NF2 である。原則として聴神経腫瘍摘出時に電極埋め込み手術を行う。腫瘍が大きく脳幹の変形が強い例では，術後の電極位置のズレを防ぐために段階手術として，電極の埋め込みを考慮したほうがよい場合もある[2]。

他にも，先天的な内耳，聴神経の形成不全の小児[3]，外傷で聴神経が切断された場合，あるいは，両側内耳の完全骨化なども適応となり，人工内耳が適応されない症例の救済手術としての大きな発展性が考えられる。

ガンマナイフ治療例では CN の神経節数が減少するために良好な成績が得られない可能性があるが，まったく適応とされないわけではない。

聴神経が保存された場合には高度難聴となっても人工内耳治療によって良好な語音聴取能が得られることがすでに報告されている[4]ので，この場合には，人工内耳治療を優先すべきである。